International Journal of Advanced Structural Engineering (2022) 12 : 647–663

ORIGINAL RESEARCH

# Seismic Evaluation of Tall Buildings with End Shear Walls by Fragility Curve

Ali Kheyroddin*[1], Mehran Akhavan Salmassi[2], Ali Hemmati[3]

**Abstract:**

Lateral bearing systems affect tall structures' behavior against lateral forces. Shear walls are one of the influential structural members against lateral forces. However, the ends of shear walls undergo severe stress under lateral forces connected to a reinforced concrete shear wall called end shear wall to improve the end structure behavior of the shear walls. Adding the end shear wall by joining the ends of the shear walls strengthened the roof rigidity and decreased the stress intensity at the concrete core end. This study modeled two 30-story concrete structures with frame and reinforced concrete shear walls with and without end shear walls to evaluate the end shear walls' behavior. First, the structure members were simulated in OpenSees to check the non-linear behavior. Then, the structures were subjected to remote domain records to examine the fragility curves. The results indicated that the end shear wall increased the maximum acceleration at maximum probability in low, medium, severe, and complete collapse states by 50, 28, 27, and 38%, respectively. The fragility curves showed a more appropriate behavior of the 30-story structure with end shear walls in low, medium, high, and complete damage states. This system is more efficient than others since the end shear wall cuts the initial period of the structure in half (from 4 to 2s in a 30-story structure with an end wall). This drastic decrease can add stories to the building. Stairs and elevators can be built into the structure instead of the end shear wall for more flexibility.

**Keywords:**

Tall buildings, Fragility curve, Reinforced concrete shear wall, Incremental dynamic analysis, End shear wall.

✉ Corresponding author kheyroddin@semnan.ac.ir

1. Professor of structural engineering, Faculty of Civil Engineering, Semnan University, Iran
2. Ph.D. Candidate of Structural engineering, Department of Civil Engineering, Semnan Branch, Islamic Azad university, Semnan, Iran.
3. Assistant Professor of structural engineering, Department of Civil Engineering, Semnan Branch, Islamic Azad university, Semnan, Iran.

## 1. Introduction

The researchers have suggested various methods for lateral load systems. On the other hand, seismic behavior has a significant role in high-rises. RC shear walls cause suitable performance in structures, and some studies have examined shear walls in RC structures as follows:

Some researchers have investigated RC tall buildings under extreme load and vulnerability. The authors suggested some methods to prevent progressive collapse [1]. In addition, another study on tall buildings assessed the development of earthquake vulnerability functions [2]. Another paper explored nonlinear shear walls and seismic analysis, and the results were appropriate for further numerical in tall buildings [3]. Furthermore, other researchers have modified the response spectrum in tall RC buildings. The proposed method showed good agreement with results from NLRHA [4]. Another study indicated the behavior of tall RC buildings. The result showed suitable performance related to the uplift foundation [5]. There are other studies regarding the design of tall buildings. The above paper presented the performance-based method's research and practice characteristics [6]. Other investigations about the nonlinear analysis of the 40-Story in Los Angeles have shown the inelastic flexural response at the spandrel beams over the building height and the first few levels of the core wall segments [7].

An analysis of flanged shear walls showed that the ultimate strength in the smeared model is 10% more than the discrete model [8]. The dynamic analysis in RCC buildings and the square shape shear wall was the most effective in P-Δ [9]. An evaluation of pushover analysis showed that the modal pushover analysis method is more accurate than another one in shear walls [10]. Other investigations have focused on the nonlinearity of a tube in a tall building, and some results have indicated that NLFEA in a tube building performs well [11]. Furthermore, a modal pushover analysis of the tall buildings showed estimations directly from the elastic design spectrum [12]. Some researchers have evaluated tall RC core buildings' recommendations for general modeling issues [13]. Others have studied the seismic behavior of the end walls in tall buildings. The end shear walls significantly improved the seismic behavior of the high-rises [14] [33]. The effect of ground motion on RC shear walls indicated that long-duration records caused larger collapse probabilities [15]. Others have searched about the design of shear walls in tall buildings. The designed structure was analyzed using a nonlinear static analysis procedure [16]. Others have examined the design of shear walls in tall buildings and analyzed them by a nonlinear static analysis procedure [16]. The seismic capacity of tall buildings was investigated by finite element modeling, and the results showed that the foundation uplift was not significantly affected [17]. The researchers have realized that this distribution transferred to lower stories of buildings increasing input energy [18].

Other studies have evaluated RC core walls in tall buildings and showed a 9–10% and 5–6% collapse probability of the building under near- and far-field ground motions, respectively [19]. The nonlinear fiber was analyzed in RC shear wall under earthquake records. The results showed that Rayleigh damping did not produce an accurate response [20]. The seismic performance showed the importance of effective frequency content of records in a high-rise with an RC shear wall [21].

Others have searched for plastic zone levels in RC shear walls and realized that balancing curvature demands a reduction resistance moment at the wall base. The reinforced ratio makes it possible [22]. Some researchers have focused on optimization in shear walls and found an evolutionary algorithm [23]. The effect of irregularity on the seismic design was assessed in tall buildings [24]. A numerical investigation of shear walls indicated that the shear walls had suitable rehabilitation by increasing the compressive strength of concrete materials [25]. The shear wall configuration and seismic performance of multi-story showed a 33.20% reduction of base shear by some configurations [26]. The T- some researchers have investigated shaped RC shear walls. The test results indicated better ductility of T-shaped shear walls than traditional shear walls [27]. Some researchers have noted the seismic performance of RC shear walls. The NDA and CSM methods showed suitable performance for

evaluation [28]. Others have investigated the nonlinear analysis of shear walls. Thus, explicit elastic and plastic rotations should be identified for designing the shear walls [29]. Others have examined the nonlinear dynamic response in a tall building.

The post-yield story's shear force distribution changed compared to the large and medium pulses ground motions [30]. Researchers have also looked into the topic of open-ended shear walls. They figured out that residual displacement of ESWO (end shear wall with opening) was the outcome of performing ESWO effectively at maximum displacement. Here, we see the roof's residual displacement in the X-axis, represented by three recordings. Considering the values for residual displacement [31], the ESWO improved them by as much as 67%.

An examination of end shear walls subjected to wind pressure was conducted. By comparing the tension contours, they found that CMF2 and CMF4 constructions had significantly less tension, demonstrating the usefulness of end walls under wind load [32]. A novel approach for seismic evaluation of coupled shear walls was recently presented. The performance of the described system was shown to be superior to that of a traditional coupled-wall system [34]. Some people looked into a 253-foot tower. According to the findings, the average earthquake ground motion that triggers initial collapse occurs at a rate of 8 x 105 per year, which is orders of magnitude lower than the 2475-year ground motion rate [35].

Furthermore, a tall-building seismic-resilience assessment was provided. At both the SLE and DBE levels, the effect of nonstructural components on seismic resilience exceeds that of structural components [36]. Some studies analyzed tall-building collapse records from quite close to the ground. The conditions for weaker intensity measures [37] were met by the structures studied in the H+V state, as shown by the results. Research taking SSI into account has revealed that SSI is common for buildings on soft soil and could alter their fragility [38]. A study looked for the most appropriate ground motion intensity metric for seismic evaluation in tall buildings. Higher modes and period softening [39] were found to alter the effectiveness and sufficiency of the IM Sa(T) with increasing periods T. Researchers using machine learning to evaluate the safety of reinforced concrete buildings found that the Artificial Neural Network (ANN) algorithms Extra-Trees Regressor (ETR), Extremely Randomized Tree Regressor (ERTR), Bagging Regressor (BR), Extreme Gradient Boosting (XGBoost), and Histogram-based Gradient Boosting Regression (HGBR) performed best. In addition, the Graphical User Interface (GUI) was developed as a simple yet reliable tool for evaluating the seismic risk of RC structures [40]. The seismic risk is greatly exacerbated by using a soft storey, according to the Seismic vulnerability evaluation of RC high-rise buildings, taking soil-structure interaction effects into account [41]. The largest IDR gets focused on the first level. Some people looked for New dual-pinned self-centering linked CLT shear walls: seismic design and performance evaluation. As seen in the results, the prototype building's DSCWs are up to snuff in terms of seismic performance, as defined by FEMA P695 [42]. Nonlinear time history analysis of an irregular RC building on sloping land was the topic of a recent inquiry. According to the findings, putting L-shaped shear walls in the corners can prevent structural parts from failing. Buildings with a Step-back Set-back configuration have been found to work well on hilly terrain [42].

According to the literature review, an investigation of the effect of end shear walls on the nonlinear behavior of RC tall buildings is needed. End shear walls connect the end of shear walls in all stories in tall buildings. Further, some parameters such as drifts, play a significant role in the behavior of RC tall buildings under seismic forces. Therefore, this study evaluated the effect of end shear walls with a focus on a mentioned parameter in RC tall buildings subjected to seismic load by fragility curves.

## 2. Theoretical modeling

### 2-1-List of notations

In addition, torsion is one of the most critical parameters in shear walls regarding high-rise buildings. The shear wall systems are rigid at the core base and have torsions at the top. In Fig 1(a) [44], the walls are symmetrical about the X and Y axes assuming a simple cross-section I under the torsion of the eccentric ratio (0.05), in which the warping effect is observed (ASCE7-16 (2017)). The Z-axis and wings rotate around the shear center and the X- and vertical axes, respectively, by applying the torsion T around and above the Z-axis. A moment effect occurs when the slab sections rotate around the X-axis in different directions while the plate sections are exited from the plate or warped. [44] noted that the torsion is tolerated by the spin of the wings equal to (see Figs. 1(a)- (b)- (c)- (d)):

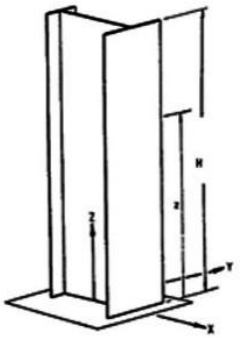

(a) Core with I section

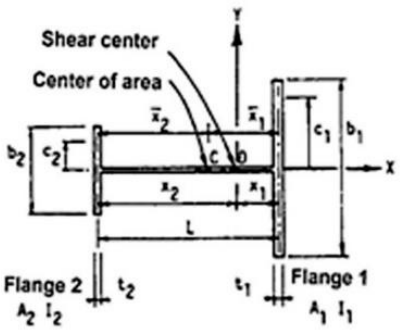


(b) Core section

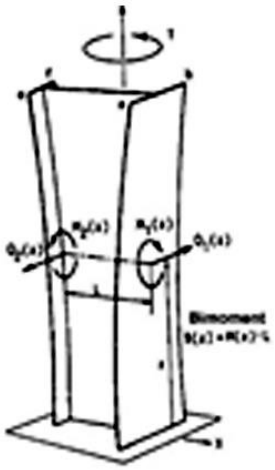

(c) Core under torsion

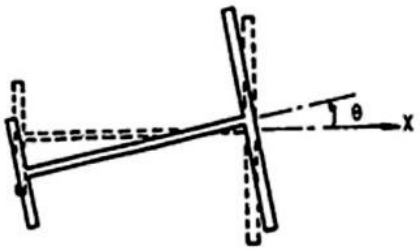


(d) Rotation of web and flanges

Fig. 1. Simple cross-section, I [44].

In Fig. 1b, $\overline{x_1}$, $\overline{x_2}$, $x_1$, and $x_2$ are the area and shear center (C and D points) as below:

$$\overline{x_1} = \frac{A_2}{A_1+A_2} L \quad \overline{x_2} = \frac{A_2}{A_1+A_2} L \tag{1}$$

$$x_1 = \frac{I_2}{I_1+I_2} L \quad x_2 = \frac{I_1}{I_1+I_2} \mathrm{L} \tag{2}$$

Vlasov's theory investigated torsion (Figs. (1c)- (1d)), which is as follows:

$$T(z) = T_v(z) + T_w(z) \tag{3}$$

$T(z)$ and $T_w(z)$ represent torsion related to warping and shear flow, respectively. In addition, Fig. 1c shows shear related to flange moments 1 and 2 by Eqs. (5)-(6):

$$Q_1(z) = -EI_1 x_1 \frac{d^3\theta}{dz^3}(z) \tag{4}$$

$$Q_2(z) = -EI_2\, x_2 \frac{d^3\theta}{dz^3}(z) \quad (5)$$

$$T_w(z)=Q_1(z)x_1 + Q_2(z)x_2 \quad (6)$$

$$T_w(z)=-EI_\omega \frac{d^3\theta}{dz^3}(z) \quad (7)$$

$I_\omega$ is geometric properties of section and nominated warping constant equal to:

$$I_\omega = I_1\, x_1^2 + I_2\, x_2^2 \quad (8)$$

$T_v(z)$ is tolerated by rotations in flanges as below:

$$T_v(z)=GJ_1 \frac{d\theta}{dz}(z) \quad (9)$$

$J_1$ is the torsion constant of the section as follows:

$$J_1 = \frac{1}{3}\sum^n bt^3 \quad (10)$$

$$J_1 = \frac{b1\, t_1^3}{3} + \frac{b2\, t_2^3}{3} \quad (11)$$

$GJ_1$ expresses the torsional rigidity of the core by open section. The equation of warping torsion is given in Eq. (12):

$$-EI_w \frac{d^3\theta}{dz^3}(z)+GJ_1 \frac{d\theta}{dz}(z)=T \quad (12)$$

On the other hand, the second moment B(z) and vertical tension of the wall at distance c from the neutral axis are equal to:

$$B(z)=M(z)L \quad (13)$$

$$\sigma(c,z)=\frac{M(z)c}{I} \quad (14)$$

The warping theory of uniform core undertorsion, Vlasov's theory (Eqs. (4)-(8)-(10)), and their differential equations are presented:

$L$ presents the vertical distance of the two flanges. $m(z)$, or wide torsion along the wide axis is equal to:

$$-m(z) = \frac{d_T}{d_z} \quad (15)$$

$\alpha$ is in the position of the shear center differential equation for core warping torsion, as shown in Eq. (17):

$$\alpha^2=\frac{GJ}{EI_\omega} \quad (16)$$

$$\frac{d^4\theta}{dz^4}(z)-\alpha^2\frac{d^2\theta}{dz^2}(z)=\frac{m(z)}{EI_\omega} \quad (17)$$

Applying boundary conditions and solving the torsion of the core under m(z) is obtained in Eq. (19):

$$\theta(z)=\frac{mH}{EI_\omega}\left\{\frac{1}{(\alpha H)^4}\left[\frac{(\alpha H \sinh \alpha H+1)}{\cosh \alpha H}(\cosh\alpha z-1)-\alpha H \sinh \alpha z+(\alpha H)^2\left[\frac{z}{H}-\frac{1}{2}\left(\frac{z}{H}\right)^2\right]\right]\right\} \quad (18)$$

$$\alpha H=H\sqrt{\frac{GI}{EI_\omega}} \quad (19)$$

$$\alpha z=\alpha H\left(\frac{z}{H}\right) \quad (20)$$

Where two parameters of αH and Z/H are dimensionless [44]. Warping tensions are mentioned as follows:

$$B(z)=-EI_\omega \frac{d^2\theta}{dz^2}(z) \quad (21)$$

$B(z)$ is the second moment, which specifies the core height ,and $\omega(s)$ presents the principle of sectoral coordinate in the section. The tension distribution in height is shown below:

$$\sigma(s,z)=\frac{B(z)\omega(s)}{I_\omega} \quad (22)$$

According to the mentioned equations, especially Eq. (22), and considering the role of stress reduction by the end shear wall, improvement in some parameters indicates the proper performance of the end shear wall.

## 2-2- Specifications of structures and materials

Some 30-story buildings with the end shear wall and without the end shear wall were modeled by ETABS software to investigate the behavior of the end shear wall. The analysis was performed in three dimensions of the study of seismic

behavior. The mentioned structures included the reinforced concrete moment frame and shear wall. The dead and live load were as much as 170 and 200 kg/m$^2$, respectively. The floor was a reinforced concrete slab, and the connections of columns and shear walls were rigid at the base. The spans of the frames were 7 m, and the height of the floors were 4 m. The value of $\upsilon$, $f_c$, and $f_y$ were as much as 0.15, 50 MPa, and 400 N/mm$^2$, respectively. The frames were modeled in three dimensions. The structures were modeled by Open Sees for nonlinear analysis due to determining frame sections in ETABS software. In Fig. 2a, the shear walls are indicated by red color. In addition, the end shear walls was shown in blue color in Figs. 2b. Figs. 2c indicated the typical frame elevation of the structure with an end shear wall.

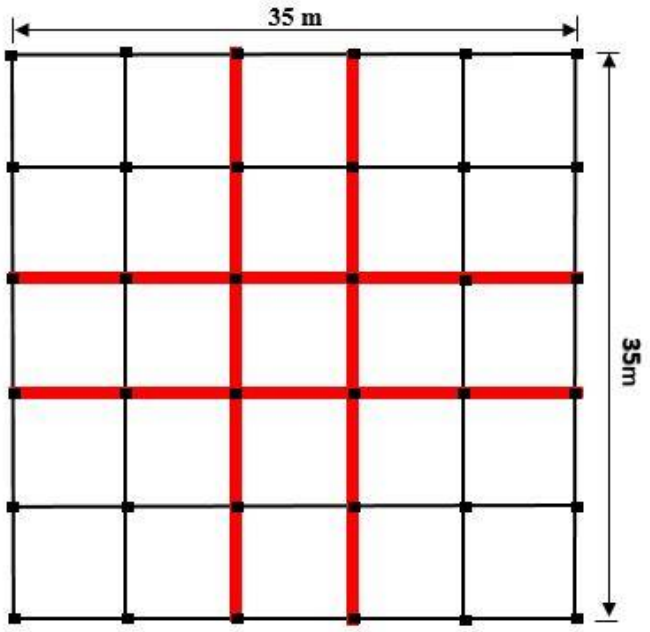


(a) The typical floor plan of structure without end shear wall

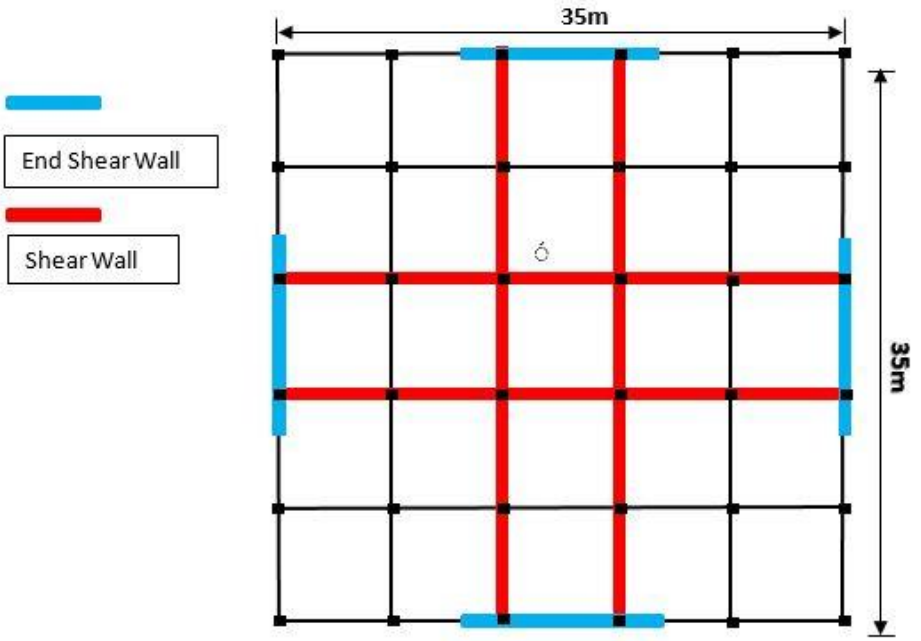


(b) The typical floor plan of structure with end shear wall

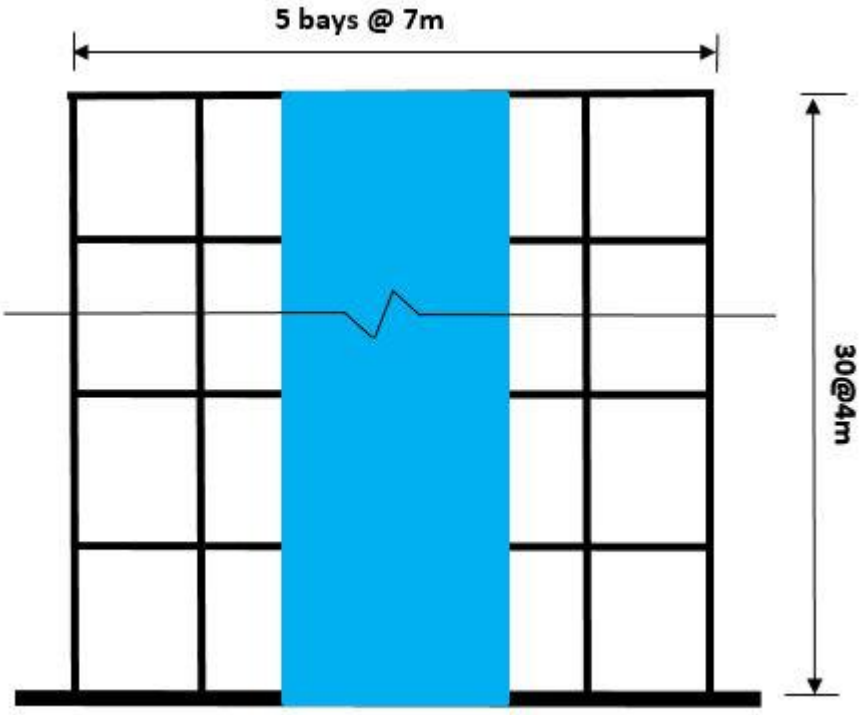


(c) The typical frame elevation of structure with end shear wall

Fig. 2. 30-story models

Table 1. Buildings specifications

| Label | H (m) | A ($m^2$) | Plan Dimensions (m×m) | Story |
|---|---|---|---|---|
| CMF1- (Without End shear wall) | 120 | 36750 | 35×35 | 30 |
| CMF2- (With End shear wall) | 120 | 36750 | 35×35 | 30 |

Table 2. Sections specifications

| Label | Dimension | Rebar |
|---|---|---|
| Beam | St1-30: (0.5) m wide × (0.7) m deep | 8$\Phi$20- Stirrup $\Phi$14@10cm |
| Column | St1-15:(1.20) m × (1.20) m, St16-30:(1.00) m × (1.00) m | 36$\Phi$32 - 36$\Phi$32 – Stirrup $\Phi$14@15cm |
| Shear Wall | St1-30:(35) m long × (0.5) m thick | $\Phi$28@10 - Stirrup $\Phi$14@25cm |
| End shear wall | St1-30:(11) m long × (0.5) m thick | $\Phi$28@10 - Stirrup $\Phi$14@25cm |
| Slab | St1-30:(0.15) m thick | $\Phi$10@10cm |

As mentioned in the figures and specifications, these structures were subjected to seismic analysis after

modeling, and the results were analyzed.

## 2-3- Simulation of structures

The 30-Story structures were analyzed by linear static analysis, and the section properties were determined by ETABS software. Open Sees simulated the mentioned structure for more investigations and nonlinear time history analysis. Three records were required to apply the structures due to nonlinear analysis.

The multi-layer shell element model was used for shear walls. The "ShellMITC4" command was related to the multi-layer shell element model, and subdivided the shear wall into enough layers. According to the dimensions and distribution of reinforcing bars, Figs. 3 and 4 indicate the different material properties and multi-layer shell elements. Based on the

physical location and direction of the bars smeared into some orthotropic layers, the stresses over a layer thickness were assumed to be consistent with those at the mid-surface of that layer [45].

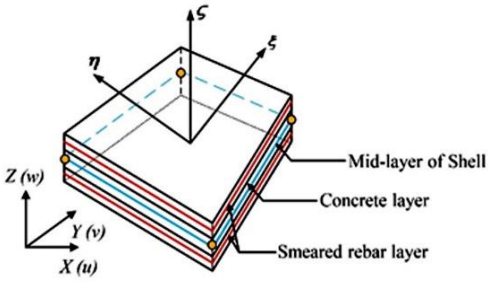


Fig. 3. Multi-layer shell element [45]

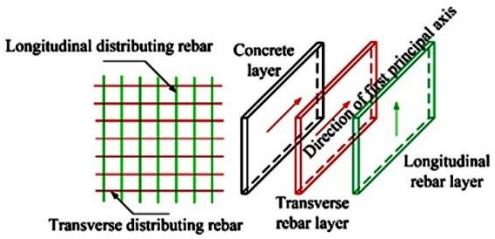


Fig. 4. Distribution of rebar layer [46].

The specifications of the records are stated in Table 3. The records were all classified as fling step and site class D.

Table 3: Fling step earthquake records specifications

| No. | Year | Earthquake | Mw | Mech.[a] | Station | Comp. | Source[b] | Site Class | PGA (g) | PGV (cm/sec) | PGD (cm) |
|---|---|---|---|---|---|---|---|---|---|---|---|
| 1 | 1999 | Kocaeli | 7.4 | SS | Yarimca (YPT) | NS | 3 | D | 0.23 | 88..83 | 184.84 |
| 2 | 1999 | Chi-Chi | 7.6 | TH | TCU052 | NS | 4 | D | 0.44 | 216 | 709.09 |
| 3 | 1999 | Chi-Chi | 7.6 | TH | TCU068 | EW | 4 | D | 0.50 | 277.56 | 715.82 |
| 4 | 1999 | Chi-Chi | 7.6 | TH | TCU074 | EW | 4 | D | 0.59 | 68.90 | 193.22 |
| 5 | 1999 | Chi-Chi | 7.6 | TH | TCU084 | NS | 4 | D | 0.42 | 42.63 | 64.91 |
| 6 | 1999 | Chi-Chi | 7.6 | TH | TCU129 | NS | 4 | D | 0.61 | 54.56 | 82.70 |
| 7 | 1999 | Chi-Chi | 7.6 | TH | TCU071 | NS | 4 | D | 0.63 | 79.11 | 244.05 |

Nonlinear analysis of structures is required in the following.

### 2-3-1- verification

A four-story RC flexural frame was studied by Para et al. (2019) and validated by Open Sees algorithms. Fig. 5a shows the detail of the Parra et al. (2019) frame [47]. In Fig. 5b, Parra et al. (2019) showed maximum base shear/W (%) and simulation graphs as a suitable verification process by Open Sees.

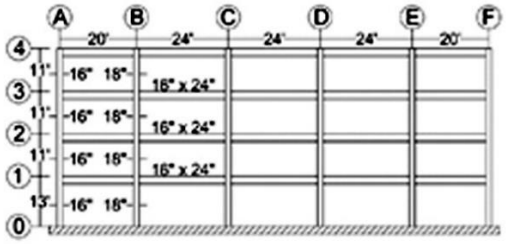

(a) The detail of Parra et al.'s frame [47]

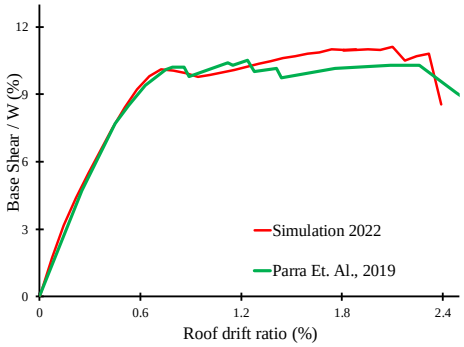


(b) Base shear/W (%)–roof drift ratio (%) graphs[47].

Fig. 5. The detail of the verification frame and results [47].

Table 4. Verification results.

| Analysis type | Maximum base shear/W (%) |
|---|---|
| Article analysis | 10.5 |
| Verification analysis | 11.1 |

As a result, the verification deviation was obtained at 5%, and Open Sees performed as expected (Table 4).

## 3. The results and discussion

The modeled 30-story structures with and without end shear walls are listed under the records in Table 3. On the other hand, the end shear wall caused a 50% reduction in the initial period of the structure (from 4s in a 30-story structure without an end wall to 2s in a 30-story structure with an end wall). Fig. 6 indicates the increasing nonlinear analysis of a 30-story structure without an end wall. Initially, the diagram was linear and in the elastic range and then entered the non-linear domain with increased structure acceleration. Behaviors such as re-hardening were observed, and finally, the structure collapsed completely with increasing intensities. Fig. 7 demonstrates the incremental nonlinear analysis for a 30-story structure with an end wall. First, the structure behaved linearly with increasing acceleration. Then, the structure entered the non-linear domain with the acceleration process, and the structure's resurrection behavior was often observed. After an earthquake reaches a certain intensity level, the structure completely collapses. According to the comparison of IDA diagrams, the end shear wall caused the structure to withstand more significant accelerations with the structural resurrection behavior. The structure reached complete collapse later. The resurrection behavior also reduced drift in the structure with the end wall.

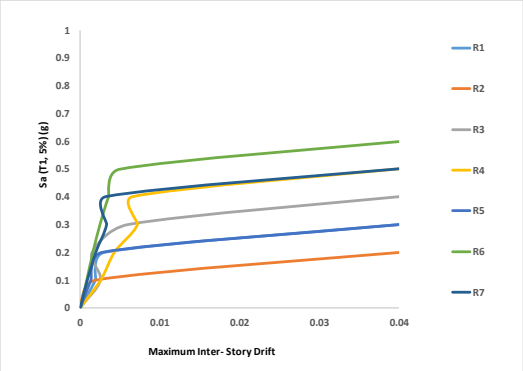


Fig. 6. IDA cure for CMF1

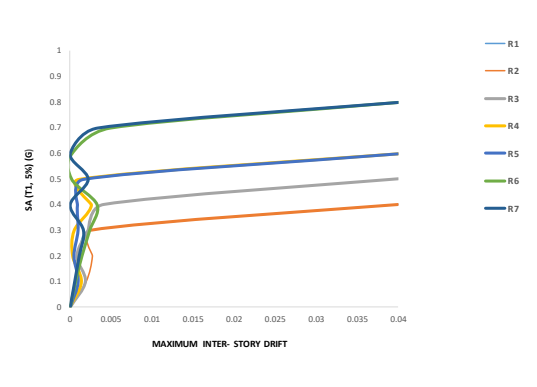


Fig. 7. IDA cure for CMF2

The average IDA graphs in two cases of 30-story structures with and without end shear walls are compared in Figure 8.

The 30-story structure with the end shear wall and resurrection behavior reduced the drift of the structure at the same accelerations. Acceleration values corresponding to the Hazus standard at different levels of damage for tall structures in slight, moderate, severe, and complete collapse states were 0.002, 0.005, 0.015, and 0.04, respectively (Figure 9). According to Figure 9, acceleration values increase from 0.1 to 0.3 in slight damage, 0.15 to 0.32 in moderate damage, 0.41 to 0.55 in severe damage, and 0.6 to 0.8 in complete collapse damage with the presence of end shear wall.

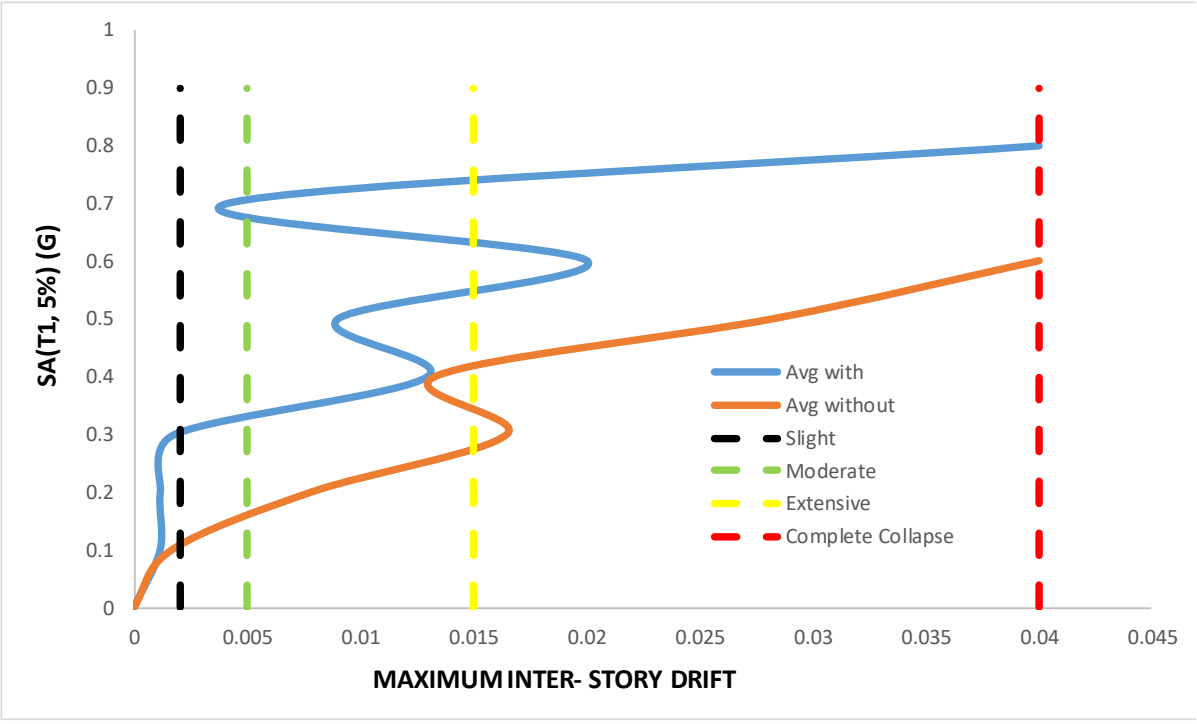


Fig. 8. Comparison of average IDA for CMF1 and CMF2.

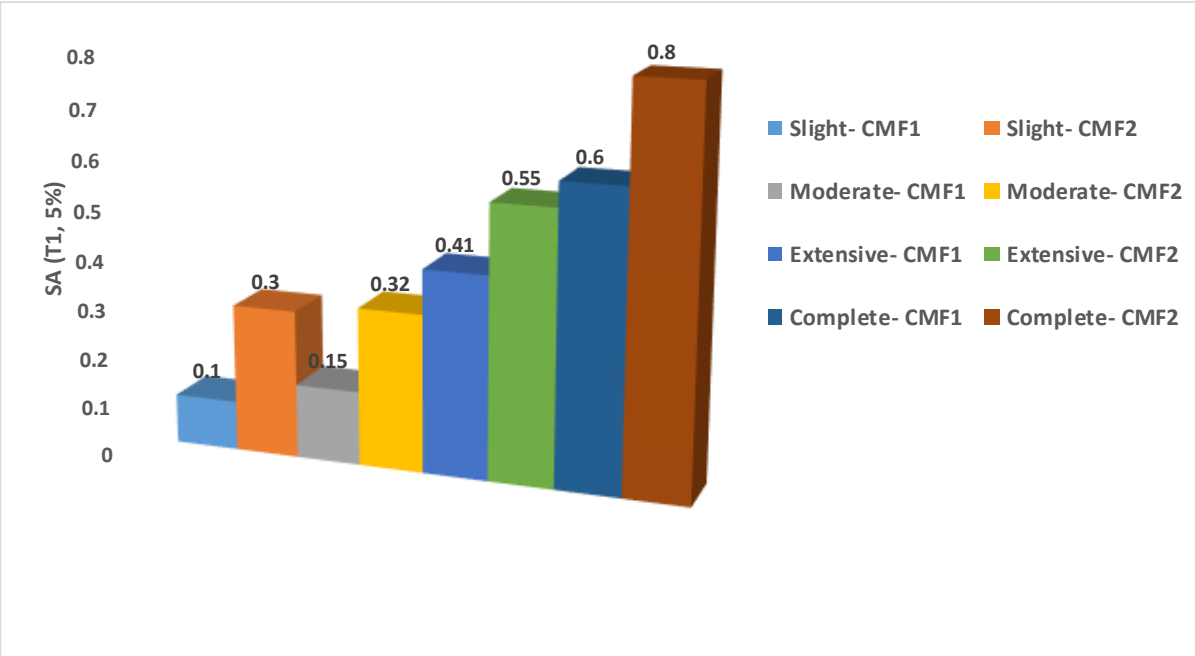


Fig. 9. Comparison The Sa (T1, 5%) of average IDA in damage states for CMF1 and CMF2.

The fragility curves of 30-story structures with and without end shear walls were drawn after examining the IDA diagram to study the behavior of the end shear wall. In Figure 10, the fragility diagram related to the structure without the end wall is considered based on Hazus standard at different levels of damage for tall structures in low, medium, severe, and complete collapse states as much as 0.002, 0.005, 0.015, and 0.04, respectively. As observed, the fragility curve for the 30-story structure with the end wall is also presented in Figure 11. The end shear wall created a uniform and parallel trend in failure levels compared to the 30-story structure without the end wall.

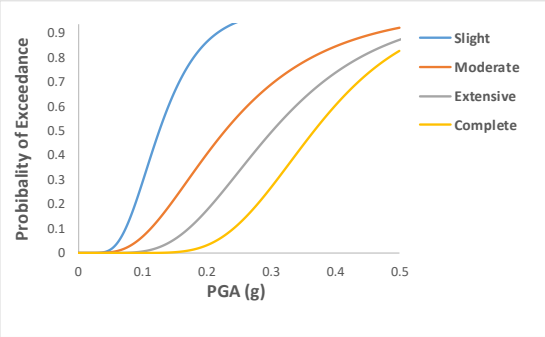


Figure 10. Fragility curve for CMF1.

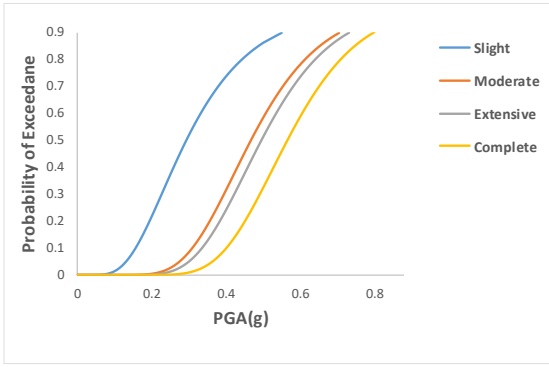


Figure 11. Fragility curve for CMF2.

Figure 12 explores different failure levels in two 30-story structures with and without end walls. The structure with the end wall had a lower probability of occurrence at the same maximum acceleration values. The maximum acceleration values at the maximum occurrence in the fragility curve for low, medium, severe, and complete collapse states were 0.25, 0.50, 0.53, and 0.5, respectively, with a 30-story structure without an end wall. These values for the 30-story structure with the end wall were 0.5, 0.70, 0.73, and 0.80, respectively, showing the structure's durability with the end shear wall under seismic behavior.

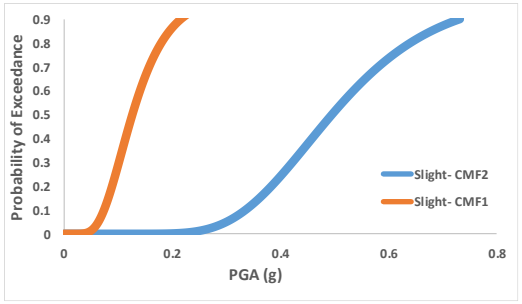


(a) Slight

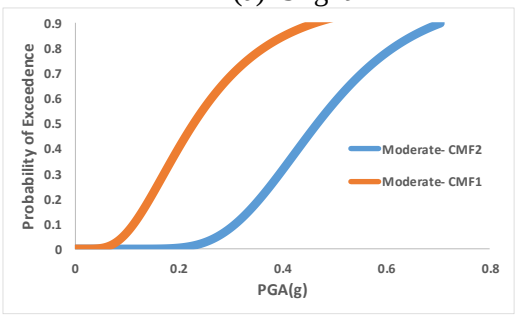


(b) Moderate

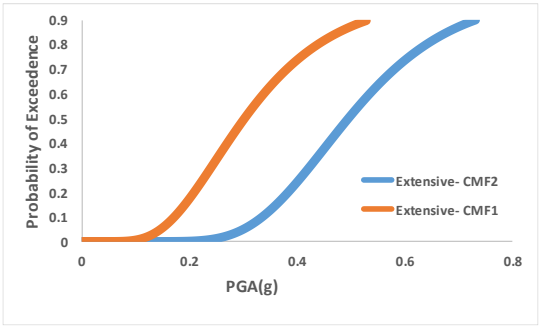


(c) Extensive

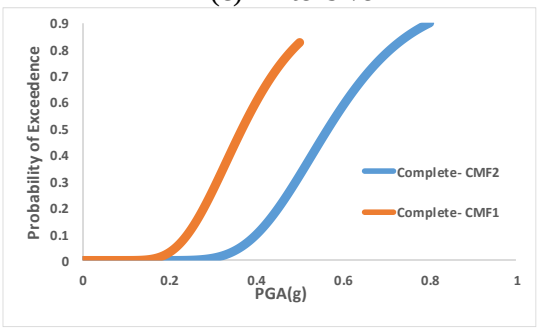


(d) Complete

Fig. 12. Comparison of different damage for CMF1 and CMF2

**Notation and symbols**

The following symbols are used in this paper:

| | |
|---|---|
| $A$ | : area of the plan |
| $B(z)$ | : second moment |
| $E$ | : young module |
| $f_c$ | : concrete comprehensive strength |
| $f_y$ | : yield strength of steel |
| $GJ$ | : torsional rigidity of the core |
| $H$ | : height of the structure |
| $I$ | : inertia moment |
| $J_1$ | : torsion constant |
| $L$ | : vertical distance of two wings |
| $M(z)$ | : wide torsion along the wide axis |
| $T$ | : torsion |
| $T_w(z)$ | : torsion associated with the warping |
| $T_v(z)$ | : torsion associated with the shear currents |
| $\alpha$ | : position of the shear center differential equation for core warping |
| $\upsilon$ | : poison coefficient |
| $\rho$ | : concrete reinforced ratio |
| $\sigma(c,z)$ | : vertical tension of the wall at a distance c from the neutral axis |
| $\sigma(s,z)$ | : Distribution of tension in height (z) |
| $\omega(s)$ | : principle sectoral coordinates |

## 4. Conclusion

This study evaluated two 30-story tall structures with and without end walls. First, two structures

were analyzed by ETABS software and then simulated with Open Sees software to check the non-linear behavior. The records of the far field were used to perform a nonlinear analysis of the structures. The results of non-linear analysis led to IDA and fragility curves, and the following results were obtained:

A. Many studies have been conducted on different layouts of shear walls. Adding the end shear wall by connecting the ends of the shear walls reduced the intensity of the stresses at the ends along the concrete core and increased the rigidity of the roofs. On the other hand, the end shear wall caused a 50% reduction in the initial period of the structure (from 4s in a 30-story structure without an end wall to 2s in a 30-story structure with an end wall), which makes this type of system more efficient than other arrangements. This significant reduction makes it possible to increase the number of floors. A staircase or elevator can also be constructed using it instead of the end shear wall.
B. According to the IDA diagrams, the end shear walls led to resurrection behavior in the structure and resulted in the complete collapse of the structure later at higher accelerations.
C. Based on the IDA diagrams, the end shear wall with structural resurrection behavior reduced drift values compared to the structure without an end wall.
D. Compared to the structure without the end wall, the damage behavior in four states of slight, moderate, severe, and complete collapse was parallel and uniform.
E. The fragility curves indicated that the maximum acceleration values at the maximum location increased the probability of occurrence in low, medium, severe, and complete collapse states by 50, 28, 27, and 38%, respectively.

Based on the results, the end shear wall outperformed the behavior of the structure and improved the seismic behavior.

## References


1. Mendis, P., Ngo, T. Vulnerability assessment of tall concrete buildings subjected to extreme loading conditions. Proceedings of the CIB-CTBUH international conference on tall buildings. 2003. 8. Pp. 10.
2. Jayaram, N., Shome, N., Rahnama, M. Development of earthquake vulnerability functions for tall buildings. Earthquake engineering & structural dynamics. 2012. 41(11). Pp. 1495–1514.
3. Lu, X., Xie, L., Guan, H., Huang, Y., Lu, X. A shear wall element for nonlinear seismic analysis of super-tall buildings using Opensys. Finite Elements in Analysis and Design. 2015. 98. Pp. 14–25.
4. Khy, K., Chintanapakdee, C., Warnitchai, P., Wijeyewickrema, A.C. Modified response spectrum analysis to compute shear force in tall RC shear wall buildings. Engineering Structures. 2019. 180. Pp. 295–309. DOI:10.1016/j.engstruct.2018.11.022. URL: https://linkinghub.elsevier.com/retrieve/pii/S0141029618316523.
5. Ugalde, D., Lopez-Garcia, D. Behavior of reinforced concrete shear wall buildings subjected to large earthquakes. Procedia engineering. 2017. 199. Pp. 3582–3587.
6. Moehle, J.P. Performance-based seismic design of tall buildings in the US. 14th World Conference on Earthquake Engineering. 2008.
7. Alwaeli, W. Framework for seismic vulnerability assessment of RC high-rise wall buildings. University of Sheffield, 2019.
8. Greeshma, S., Jaya, K.P., Sheeja, L.A. Analysis of the flanged shear wall using Ansys concrete model. International Journal of Civil & Structural Engineering. 2011. 2(2). Pp. 454–465.
9. Mohan, R., Prabha, C. Dynamic analysis of RCC buildings with the shear wall. International Journal of Earth Sciences and Engineering. 2011. 4(06). Pp. 659–662.
10. Miao, Z., Ye, L., Guan, H., Lu, X. Evaluation of modal and traditional pushover analyses in frame-shear-wall structures. Advances in Structural

Engineering. 2011. 14(5). Pp. 815–836.

11. Marsono, A.K., Wee, L.S. Nonlinear finite element analysis of reinforced concrete tube in a tube of tall buildings. Proceedings of the 6th Asia-Pacific Structural Engineering and Construction Conference (APSEC 2006). 2006. Pp. 5–6.

12. Reyes, J.C., Chopra, A.K. Three-dimensional modal pushover analysis of buildings subjected to two components of ground motion, including its evaluation for tall buildings. Earthquake Engineering & Structural Dynamics. 2011. 40(7). Pp. 789–806.

13. Wallace, J.W. Modeling issues for tall reinforced concrete core wall buildings. The structural design of tall and special buildings. 2007. 16(5). Pp. 615–632.

14. Akhavan, S.M., Kheyroddin, A., Hemmati, A. Seismic behavior of end walls in RC tall buildings with torsional irregularity. Magazine of Civil Engineering. 2020. (5). Pp. 9707.

15. Fairhurst, M., Bebamzadeh, A., Ventura, C.E. Effect of Ground Motion Duration on Reinforced Concrete Shear Wall Buildings. Earthquake Spectra. 2019. 35(1). Pp. 311–331. DOI:10.1193/101117EQS201M. URL: http://journals.sagepub.com/doi/10.1193/101117EQS201M.

16. LIANG, X., DENG, M., LI, B.O., YANG, K. Displacement-based seismic design of shear wall structure in tall buildings. Tall Buildings: From Engineering to Sustainability. World Scientific, 2005. Pp. 159–164.

17. Ugalde, D., Parra, P.F., Lopez-Garcia, D. Assessment of the seismic capacity of tall wall buildings using nonlinear finite element modeling. Bulletin of Earthquake Engineering. 2019. 17(12). Pp. 6565–6589.

18. Jamnani, H.H., Amiri, J.V., Rajabnejad, H. Energy distribution in RC shear wall-frame structures subject to repeated earthquakes. Soil Dynamics and Earthquake Engineering. 2018. 107. Pp. 116–128.

19. Emami, A.R., Halabian, A.M. Incremental dynamic collapse analysis of RC core-wall tall buildings considering spatial seismic response distributions. The Structural Design of Tall and Special Buildings. 2017. 26(15). Pp. e1383.

20. Beiraghi, H., Kheyroddin, A., Kafi, M.A. Nonlinear fiber element analysis of a reinforced concrete shear wall subjected to earthquake records. Iranian Journal of Science and Technology Transactions of Civil Engineering. 2015. 39(C2+). Pp. 409–422.

21. Afzali, A., Mortezaei, A., Kheyroddin, A. Seismic Performance of High-Rise RC Shear Wall Buildings Subjected to Ground Motions with Various Frequency. Civil Engineering Journal. 2017. 3(8).

22. Kafi, M.A. Effect of plastic zone levels on the responses of concrete shear walls subjected to strong ground motions. Authorea Preprints. 2020.

23. Zhang, Y., Mueller, C. Shear wall layout optimization for conceptual design of tall buildings. Engineering Structures. 2017. 140. Pp. 225–240. DOI:10.1016/j.engstruct.2017.02.059. URL: https://linkinghub.elsevier.com/retrieve/pii/S0141029616315115.

24. Mwafy, A., Khalifa, S. Effect of vertical structural irregularity on seismic design of tall buildings. The Structural Design of Tall and Special Buildings. 2017. 26(18). Pp. e1399.

25. Kheyroddin, A., Hajforoush, M., Doustmohammadi, A. Numerical investigation of composite shear walls with different steel and concrete materials as boundary elements. Journal of Rehabilitation in Civil Engineering. 2020. 8(3). Pp. 124–138.

26. Mahmoud, S. In-Plane Shear-Wall Configuration Effects on the Seismic Performance of Symmetrical Multistory Reinforced-Concrete Buildings. International Journal of Civil Engineering. 2021. Pp. 1–14.

27. Tosee, V.R. Soil Structure Interaction Journal (SSIJ).

28. Jeon, S.-H., Park, J.-H. Seismic Fragility Assessment of Ordinary RC Shear Walls Designed with a Nonlinear Dynamic Analysis. Journal of the Earthquake Engineering Society of Korea. 2019. 23(3). Pp. 169–181.

29. Debnath, P.P., Choudhury, S. Nonlinear analysis of shear wall in unified performance-based seismic design of buildings. ASIAN JOURNAL OF CIVIL ENGINEERING (BHRC). 2017. 18(4). Pp. 633–642.

30. Güneş, N., Ulucan, Z.Ç. Nonlinear dynamic response of a tall building to near-fault pulse-like ground motions. Bulletin of Earthquake Engineering. 2019. 17(6). Pp. 2989–3013.

31. Akhavan Salmassi, M., Kheyroddin, A. Hemmati, A. Seismic Behavior of Tall Buildings with End Shear Walls and Opening, Journal Seismology & Earthquake Engineering. 2021. Published online. https://doi.org/ 10.48303/JSEE.2023.1973892.1036

32. Akhavan Salmassi, M., Kheyroddin, A. Hemmati, A.Effect of End Walls in Tall Buildings with Square Plan and Concrete Frames under Wind Load, 12th National Congress on Civil Engineering. 2020. At: Sahand University of Technology, Tabriz, Iran.

33. Akhavan Salmassi, M., Kheyroddin, A. Hemmati, A. Effect of end walls in tall buildings with a square plan and flexural concrete frames under earthquake, 7th National and 3rd International Conference on Modern Materials and Structures in Civil Engineering. 2018. Tehran, Iran.

34. Li, S., Jiang, H., Kunnath, S.K. Seismic assessment of a new resilient coupled shear wall, Engineering Structures. 2023. 277. Pp. 115476. https://doi.org/10.1016/j.engstruct.2022.115476

35. Budak, E., Sucuoğlu, H. Cem Celik, O. Response parameters that control the service, safety, and collapse performances of a 253 m tall concrete core wall building in Istanbul. Bulletin of Earthquake Engineering. 2023. 21. Pp. 375–395

36. Lu, X., Chen, A. Quantitative evaluation and improvement of seismic resilience of a tall frame shear wall structure. Tall and Special buildings 31(1). 2021. https://doi.org/10.1002/tal.1899

37. Taslimi, A., Tehranizadeh,. M The effect of vertical near-field ground motions on the collapse risk of high-rise reinforced concrete frame-core wall structures. Advances in Structural Engineering. 2021. 25(2) .https://doi.org/10.1177/13694332211056106.

38. Pitilakis, D. Petredis, C. Fragility curves for existing reinforced concrete buildings, including soil–structure interaction and site amplification effects. Engineering Structures. 2022. 269. Pp. 114733. https://doi.org/10.1016/j.engstruct.2022.114733

39. Rong, X., Yang, J., Jun, L., Zhang, Y., Zheng, S., Dong, L. Optimal ground motion intensity measure for seismic assessment of high-rise reinforced concrete structures. Case Studies in Construction Materials.2023.18. https://doi.org/10.1016/j.cscm.2022.e01678.

40. Kazemi, F., Asgarkhani, N., Jankowski, R. Machine learning-based seismic fragility and seismic vulnerability assessment of reinforced concrete structures. Soil Dynamics and Earthquake Engineering. 2023. 166. https://doi.org/10.1016/j.soildyn.2023.107761

41. Kanth Sriwastav, R.Seismic vulnerability assessment of RC high-rise building considering soil–structure interaction effects. Asian Journal of Civil Engineering. 2022. 23. Pp. 585–608.

42. Lepine-Lacroix, S., Yang, T.Y. Seismic design and performance evaluation of novel dual-pinned self-centering coupled CLT shear walls. Engineering Structures. 2023. 279. Pp. 115547. https://doi.org/10.1016/j.engstruct.2022.115547

43. Singh, L. Singh, H. Kaur, I. Nonlinear time history analysis on irregular RC building on

sloping ground. Innovative Infrastructure Solutions. 2023. 8.

44. Smith, B.S., Coull, A. Tall building structures analysis and design. 1991. 310–329 p. ISBN:978-0-471-51237-0.

45. Lu, X. Xie, L. Guan, H. Huang, Y. Lu, X.A shear wall element for nonlinear seismic analysis of super-tall buildings using Open Sees, Finite Elements in Analysis and Design. 2015. (98). Pp. 14-25.

46. Zhu, T. Heidebrecht, A. Tso, W. Effect of peak ground acceleration to velocity ratio on ductility demand of inelastic systems, Earthquake engineering & structural dynamics. 1998. 16(1). Pp. 63-79.

47. Parra, P. Arteta, C. Moehle, J. Modeling criteria of the older non-ductile concrete frame–wall buildings, Bulletin of Earthquake Engineering. 2019. 17(12). Pp. 6591-6620.